Estimations of Surface Soil Moisture for Intertidal Mudflats Using a Near-infrared Long-Range Terrestrial Laser Scanner

Jin Chen, Kai Tan, Weiguo Zhang

State Key Laboratory of Estuarine and Coastal Research, East China Normal University

E-mail: 2431016514@qq.com

H51U-1819

Abstract

Estimations of the soil surface water contents and distributions play a key role in the ecological, environmental, and topographical investigations for intertidal mudflats. However, existing techniques have limitations. Long-range terrestrial laser scanners (TLSs) can record the co-located intensity value which refers to a measure of the backscattered laser from each scanned point. Most long-range TLSs emit near-infrared lasers that can be strongly absorbed by water. Thus, the intensity values can be used as proxies for water contents. In this study, the intensity data of long-range TLSs are corrected for the incidence angle and distance effects to quantitatively estimate the soil surface water contents of intertidal mudflats. A case study for a mudflat in Chongming Island, Shanghai, China, is conducted. Results indicate that compared with traditional techniques, the corrected intensity data of long-range TLSs are extremely effective data sources for a quick, accurate, and detailed estimation of water contents for large-area mudflats. The estimation root mean square error is approximately 3%. Furthermore, the 3D distributions of the water contents can be accurately mapped by combining the point cloud of the mudflats to potentially analyze the intrinsic association among water contents and topography, vegetation coverage, and habitation of creatures in mudflats.

Study area and Instruments

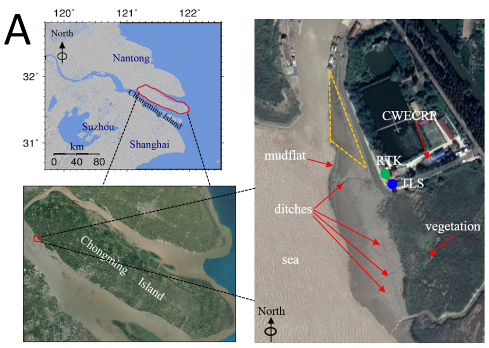

(A) Location of the study mudflat. The orthophoto of the mudflat was provided by Google Earth. Riegl VZ-4000 TLS and Trimble R8 RTK reference station were positioned at the blue and green points, respectively. The north corner of the mudflat (yellow dotted frame) cannot be scanned by the TLS.

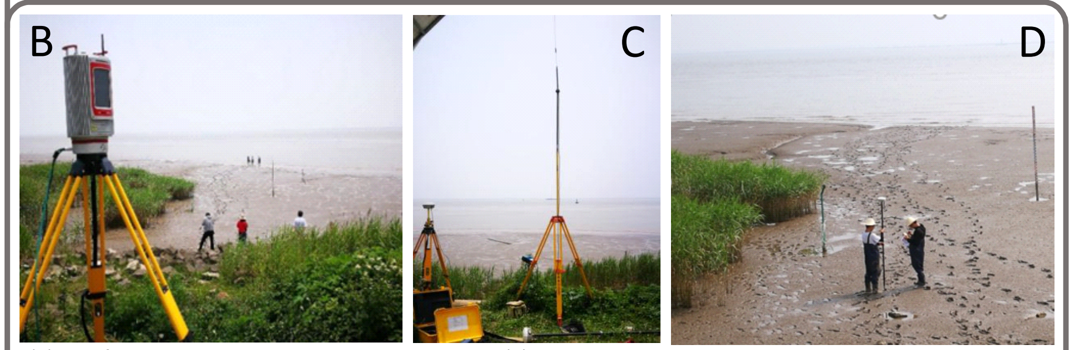

(B) Mudflat point cloud collection by Riegl VZ-4000. (C) Trimble R8 GPS RTK base station. The base station was positioned nearby Riegl VZ-4000. (D) Samples collection. The positions of the samples were measured by the RTK.

Relationship between Corrected Intensity Data and Water Contents

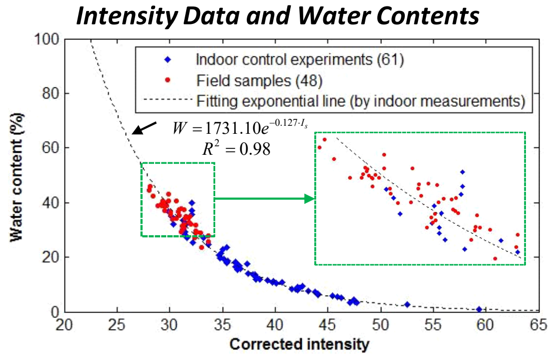

Methods

Intensity Correction

$$I = f_1(\rho)\cdot f_2(\theta)\cdot f_3(d) \quad (1)$$

$$\begin{cases} \theta = \cos^{-1}\left|\dfrac{OS\cdot n}{d\cdot|n|}\right| \\ d = \sqrt{(x-x_0)^2+(y-y_0)^2+(z-z_0)^2} \end{cases} \quad (2)$$

$$I_s = f_1(\rho)\times f_2(\theta_s)\times f_3(d_s) \quad (3)$$

$$I_s = I\cdot\frac{f_2(\theta_s)\cdot f_3(d_s)}{f_2(\theta)\cdot f_3(d)} = I\cdot\frac{\sum_{i=0}^{N_2}(\alpha_i\theta_s^i)\cdot\sum_{i=0}^{N_3}(\beta_i d_s^i)}{\sum_{i=0}^{N_2}(\alpha_i\theta^i)\cdot\sum_{i=0}^{N_3}(\beta_i d^i)} \quad (4)$$

Equation(4) was used to correct the incidence angle and distance effect of intensity data. The above methods were used in Tan et al.

Estimation of Polynomial Parameters

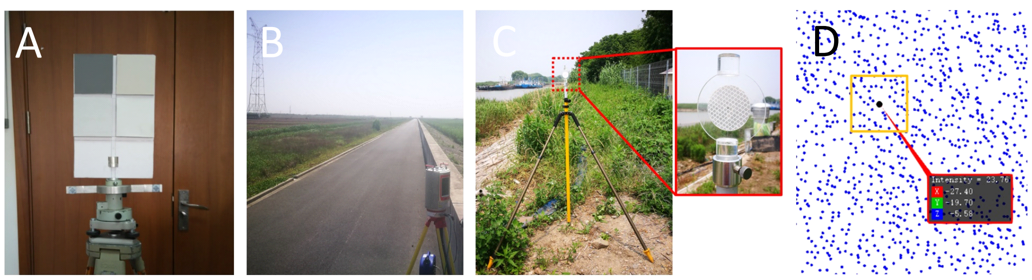

Estimation of Water Contents Using Corrected Intensity Data

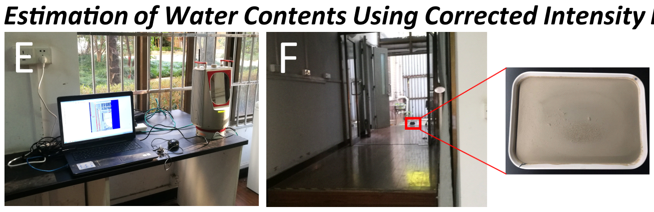

(F) Sediment sample, the distance from scanner was about 10 m.

(A) Four different homogeneous targets.
(B) A cement road.
(C) One of the plastic targets used to match the data acquired by Riegl VZ-4000 and Trimble R8 GNSS RTK.
(D) Calculation of the corrected intensity values for the field samples.
(E) Riegl VZ-4000 used to scan the new sample in indoor environments.

Results

Polynomial Parameters Estimation for TLS Intensity Correction

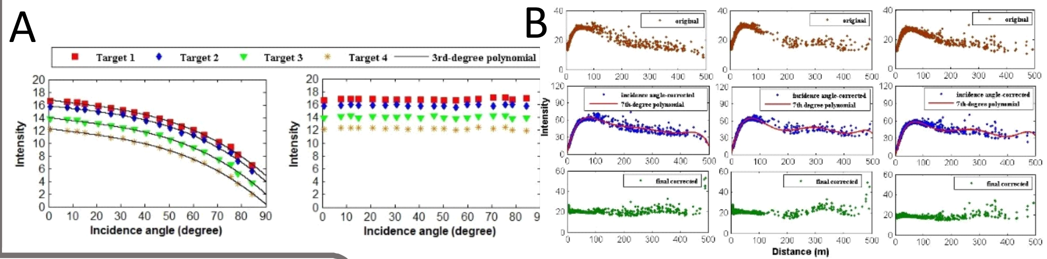

(A) Experimental results between the incidence angle and original intensity of the four reference targets. (B) Final corrected data by the improved method

C

N_2	$\alpha_0/\sigma_{\alpha_0}$	$\alpha_1/\sigma_{\alpha_1}$	$\alpha_2/\sigma_{\alpha_2}$	$\alpha_3/\sigma_{\alpha_3}$
3	1.00/0.14	$-3.38\times10^{-3}/0.73$	$2.4\times10^{-5}/1.2$	$-9.73\times10^{-7}/0.50$
N_3	β_0/σ_{β_0}	β_1/σ_{β_1}	β_2/σ_{β_2}	β_3/σ_{β_3}
7	$-7.49\times10^{-2}/0.84$	2.55/0.62	27.6/1.4	140.0/1.4
β_4/σ_{β_4}	β_5/σ_{β_5}	β_6/σ_{β_6}	β_7/σ_{β_7}	
−377.5/1.9	552.08/0.74	−394.4/1.8	1.00/0.22	

(C) Polynomial parameters and standard deviations.

Estimation of Mudflat Water Contents Using Corrected Intensity Data

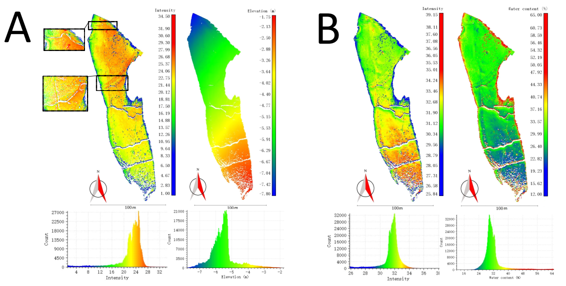

(A) Point cloud of the study mudflat colored by original intensity(left figure); Point cloud colored by elevation(right figure); Histogram of the original intensity data and the elevation(following figure).
(B) Point cloud of the study mudflat colored by corrected intensity data(left figure); Point cloud colored by water content(right figure); Histogram of the corrected intensity data and the water contents(following figure).

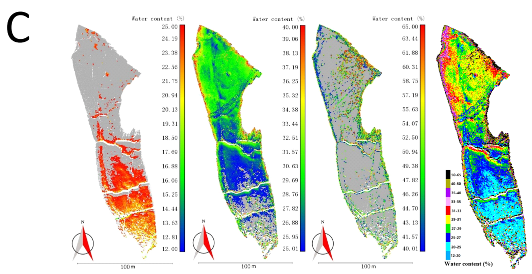

(C) Water content 12%-25%(low), 25%-40%(middle), 40%-65%(high) estimated by corrected intensity data, and water contents segmented into 10 sections.

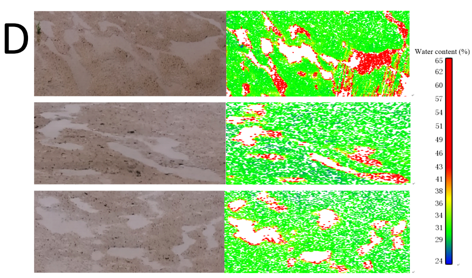

(D) Local low-lying areas with high water contents. Left: RGB images taken on site; right: Estimated water contents.

Error Calculation

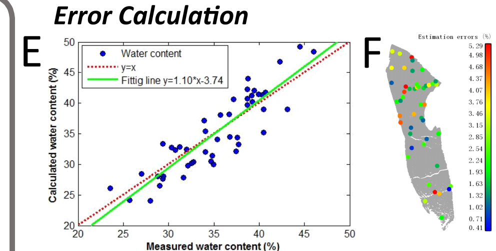

(E) Relationship between the measured water contents by gravimetric method and calculated water contents by corrected intensity data for the 48 field samples. (F) Spatial distribution and water contents estimation errors for the 48 field samples.

Conclusions

1. Incidence angle and distance significantly affect the intensity data of long-range TLSs.
2. The relationship between water contents and corrected intensity data can be modelled by an exponential model where the RMSE is approximately 3%.
3. Regions with high level water contents lie at the edges between mudflat and sea water, local low-lying areas, shores of ditches, and edges between the vegetation and mudflat.

Acknowledgments

This research is funded by East China Normal University Graduate Student Funding for International Conferences and Ministry of Science and Technology of the People's Republic of China under Grant 2017YFE0107400.